

## Study of Spectral Reflectance Reconstruction Based on an Algorithm for Improved Orthogonal Matching Pursuit

Zhang Leihong<sup>1</sup>, Liang Dong<sup>1\*</sup>, Zhang Dawei<sup>2</sup>, Gao Xiumin<sup>2</sup>, and Ma Xiuhua<sup>3</sup>

<sup>1</sup>College of Communication and Art Design, University of Shanghai for Science and Technology, Shanghai 200093, China

<sup>2</sup>School of optical electrical and computer engineering, University of Shanghai for Science and Technology, Shanghai 200093, China

<sup>3</sup>Shanghai Institute of Optics and Fine Mechanics, CAS, Shanghai 201800, China

(Received January 11, 2016 : revised May 12, 2016 : accepted June 2, 2016)

Spectral reflectance is sparse in space, and while the traditional spectral-reconstruction algorithm does not make full use of this characteristic sparseness, the compressive sensing algorithm can make full use of it. In this paper, on the basis of analyzing compressive sensing based on the orthogonal matching pursuit algorithm, a new algorithm based on the Dice matching criterion is proposed. The Dice similarity coefficient is introduced, to calculate the correlation coefficient of the atoms and the residual error, and is used to select the atoms from a library. The accuracy of Spectral reconstruction based on the pseudo-inverse method, Wiener estimation method, OMP algorithm, and DOMP algorithm is compared by simulation on the MATLAB platform and experimental testing. The result is that spectral-reconstruction accuracy based on the DOMP algorithm is higher than for the other three methods. The root-mean-square error and color difference decreases with an increasing number of principal components. The reconstruction error decreases as the number of iterations increases. Spectral reconstruction based on the DOMP algorithm can improve the accuracy of color-information replication effectively, and high-accuracy color-information reproduction can be realized.

**Keywords :** Compressive sensing, Orthogonal matching pursuit, Dice coefficient, Principal component analysis, Spectral reconstruction

**OCIS codes :** (270.5585) Quantum information and processing; (300.6170) Spectra; (300.6490) Spectroscopy, surface

### I. INTRODUCTION

Multispectral image-replication technology always uses the spectral reflectance instead of RGB or CMYK color values for the processing and reproduction of color information, to avoid the change in the characteristics of spectral image color with external conditions and human vision. An image's color information is affected by external conditions such as the light source, but the spectral-reflectance information on the surface of the object is not affected by external conditions, and can truly reflect the surface's color information.

At present, multispectral imaging systems mainly use principal component analysis (PCA) [1, 2], independent component analysis (ICA) [3] and Wiener estimation method [4], or the pseudo-inverse method [5] to reconstruct the spectral reflectance of an image surface, with limited accuracy. Compressive sensing theory [6-14] can make full use of signal sparsity and reconstruct the signal accurately, under the condition that the sampling rate is lower than that of the Nyquist requirement. Spectral reflectance is a sparse signal, but traditional reconstruction algorithms do not make full use of this characteristic sparsity. The compressive

\*Corresponding author: [ldusst@163.com](mailto:ldusst@163.com)

Color versions of one or more of the figures in this paper are available online.



This is an Open Access article distributed under the terms of the Creative Commons Attribution Non-Commercial License (<http://creativecommons.org/licenses/by-nc/3.0/>) which permits unrestricted non-commercial use, distribution, and reproduction in any medium, provided the original work is properly cited.

Copyright © 2016 Optical Society of Korea

sensing algorithm can make full use of the sparsity of the spectral reflectance, and thus reduce the number of calculations and computing time. This paper uses an improved orthogonal matching pursuit algorithm to reconstruct the spectral reflectance of the image surface. On the basis of analyzing the orthogonal matching pursuit algorithm, the correlation coefficient of atoms and the residual error are calculated, and the Dice similarity coefficient is introduced and used as a new principle to select atoms from the atom library. Thus it can improve the accuracy of color-information replication effectively, and high-accuracy reproduction of color information can be realized.

### 1.1. Compressive Sensing Principle

Compressive sensing theory breaks from traditional Nyquist sampling theory, and uses a small number of sample points to restore the original signal. Compressive sensing theory is based on the sparse signal representation and the incoherence of signal measurement. If the coefficient of the basis vector of a signal consists of a large number of zero elements, the signal is sparse. Most signals in nature are not sparse, but can have a sparse representation, after some transformation. In some transformation domain, the signal is sparse. A finite, one-dimensional discrete signal of length  $N$  can be expressed as:

$$x = \psi s \quad (1)$$

where  $\psi$  is the basis vector and  $S$  is the weighting coefficient of the basis vector. To reconstruct the signal  $x$ ,  $x$  it must be measured  $M$  ( $M < N$ ) times. The process can be expressed as the following:

$$y = \phi x = \phi \psi s \quad (2)$$

where  $\phi$  is measurement matrix of dimensions  $(M \times N)$ , and  $y$  is the linear measurement value of length- $N$  signal  $x$ . Apparently the dimension of  $y$  is far smaller than that of the signal  $x$ . Eq. (2) has no solution; it is an ill-posed problem, and it is difficult to reconstruct the original signal. If the original signal  $x$  is  $K$ -sparse, and the  $\psi$  and  $\phi$  are incoherent, then the signal  $x$  can be reconstructed accurately with measurement value  $y$  by solving the optimization problem of  $l_1$  norm.

$$\hat{s} = \arg \min \|s\|_{l_1}, y = \phi \psi s = \Theta s \quad (3)$$

In Eq. (3),  $\|\cdot\|_{l_1}$  is the  $l_1$  norm of the vector,  $\Theta = \phi \psi$  is the sensing matrix of dimensions  $M \times N$ , and  $y$  is the measurement value of the sparse signal  $x$  by the measurement matrix  $\phi$ .

## II. SPECTRAL REFLECTANCE RECONSTRUCTION BASED ON THE IMPROVED OMP ALGORITHM

### 2.1. Spectral Reflectance Reconstruction Based on the Pseudo-inverse Method

When the spectral imaging system operates, the output image channel value is affected by the relative spectral energy distribution of the standard lighting  $I(\lambda)$ , the spectral reflectance  $r(\lambda)$  of the image, the sensitivity of the camera  $s(\lambda)$ , and the spectral transmittance of the color filter  $\tau_k(\lambda)$ . The process is shown in Eq. (4):

$$u_k = \int_{\lambda_{min}}^{\lambda_{max}} s(\lambda) I(\lambda) r(\lambda) \tau_k(\lambda) d\lambda \quad (4)$$

where  $k$  is the channel number and  $u_k$  is the output image signal of channel  $k$  of the spectral imaging system. Eq. (4) can be expressed as a discrete matrix:

$$u_k = M^T r \quad (5)$$

where  $M^T$  represents the spectral response matrix.  $Q = M(M^T M)^{-1}$  can be obtained by the least-squares method  $\min \|Qu - r\|_2^2$ , and then the spectral reflectance can be obtained by the following formula:

$$r = M(M^T M)^{-1} u_k \quad (6)$$

### 2.2. The Improved OMP Algorithm

The OMP (orthogonal matching pursuit) algorithm uses iterative-algorithm thought to reconstruct the signal. In each iteration, the correlation coefficient is calculated by seeking the absolute value of the inner product of each atom among atom libraries (the sensing matrix  $\Theta$ ) and the residual error  $r_i$ , as shown in Eq. (7).

$$\mu = \{\mu_j | \mu_j = |\langle \Theta_j, r_i \rangle|, j = 1, 2, \dots, N\} \quad (7)$$

Where, atom means a primitive component of the reconstruction. Then, through the correlation coefficient  $\mu$ , from the library the atom positions that best matched the signal are found. The index set is updated, and from the atom library the column that best matched the residual error is chosen to constitute a new matrix  $\Theta_{T_i}$ , the support set. Through the support set  $\Theta_{T_i}$  and the measured values  $y$ , the estimated value of the sparse signal  $S$  is obtained by the least-squares method. After such iteration, the final reasonable sparse coefficient  $\hat{S}$  is obtained.

$$\hat{s} = \arg \min \|y - \Theta s\|_2 \quad (8)$$

Unlike the previous OMP algorithm, in which the correlation coefficient of each atom and the residual error is computed, an improved OMP algorithm called the DOMP algorithm (DOMP is short for an improved orthogonal matching pursuit algorithm, based on the matching criterion of the Dice coefficient.) introduces the Dice similarity coefficient, which is a new principle for selecting an atom from the atom library. For any two vectors  $\alpha$ ,  $\beta$  the Dice coefficient is:

$$Dice(\alpha, \beta) = \frac{2 \sum_{i=1}^n \alpha_i \beta_i}{\sum_{i=1}^n \alpha_i^2 + \sum_{i=1}^n \beta_i^2} \quad (9)$$

where  $\alpha = (\alpha_1, \alpha_2, \dots, \alpha_n)$ ,  $\beta = (\beta_1, \beta_2, \dots, \beta_n)$ . Eq. (9) represents the Dice matching coefficient of  $\alpha$ ,  $\beta$ . Instead of the geometric mean, the Dice coefficient criterion uses in the denominator the arithmetic mean values of the sum of squares of each component of each vector. Because the arithmetic mean values can highlight the important components of the vectors effectively and accurately, the atoms that best match the residual signal can be accurately selected from the sparse dictionary, using the Dice coefficient criterion.

The principle of selecting the optimal atom is shown as  $\lambda_t = \arg \max_{j=1,2,\dots,N} |D(r_{t-1}, \Theta_j)|$ , where  $\lambda_t$  is the index position of selected atoms in the atom library, and  $D(r_{t-1}, \Theta_j)$  represents the Dice similarity coefficient of residual error and each atom. Then  $T_t = T_{t-1} \cup J_0$ ; Introducing the Dice coefficient in DOMP algorithm allows the updated modulus of residual error to be small, and the larger coefficient of a vector to be more prominent; then it can pinpoint the important parts of the residual error rapidly and accurately via the DOMP algorithm.

In the OMP algorithm, when using inner product to measure the similarity criterion, the important part of the signal has not been significantly enlarged. Thus how to choose atoms better matching the residual signal is studied in this paper, and optimization of the support set is realized by introducing the Dice coefficient matching measurement standards, instead of inner product standards. In Eq. (9), the Dice coefficient can make full use of each element of the vector to calculate the correlation, and the role of each element of the vector when calculating the correlation is magnified. The important role of each element in the selection of atoms is reflected, so the performance of the DOMP algorithm is superior to that of the OMP algorithm.

### 2.3. Spectral Reflectance Reconstruction Based on DOMP Algorithm

The spectral-reflectance reconstruction based on the DOMP algorithm uses a principal component analysis algorithm to obtain a basis function vector from the training samples, and sets the first three principal components to be the basis function vector for spectral-reflectance reconstruction of the test sample. According to the smoothness of the spectral

reflectance,  $r$  is linearly combined with a feature vector of dimension  $J$ . If the spectral reflectance  $r$  is evenly sampled  $N$  times, the linear model can be expressed as:

$$r = Ba = [b_1, b_2, \dots, b_J][a_1, a_2, \dots, a_J]^T \quad (10)$$

$r$  is an  $N \times 1$ -dimensional spectral reflectance vector,  $B$  is an  $N \times J$ -dimensional basis function vector matrix, and  $a$  is a  $J \times 1$ -dimensional coefficient of the basis function vector. According to the above analysis, Eq. (5) can be expressed as:

$$u_k = M^T r = M^T Ba \quad (11)$$

$u_k$  is a  $K$ -dimensional vector; because  $K < N$ , the formula (5) does not have a definite solution.  $r$  can be expressed as  $r = Ba$ ; then the  $r$  is a  $J$ -sparse vector. If  $J < K$ , Eq. (5) will have a definite solution.  $B = (b_1, b_2, b_3)$  is obtained by the principal component analysis algorithm, the coefficient  $a$  is obtained by the DOMP algorithm, and the spectral reflectance of test samples  $\hat{r}$  is reconstructed by the DOMP algorithm.

$$\hat{r} = B \left\{ \arg \min_a \|u_k - M^T Ba\|_2 \right\} \quad (12)$$

$\hat{r}$  represents the reconstructed spectral reflectance, while  $u_k$  represents the channel response value of the test sample.

In the sensing process, the Dice coefficient is introduced to change the matching criterion for sparse dictionary atoms and the residual signal, and compared with the OMP algorithm, and then the support set is optimized. Therefore, the atoms that best match the residual error can be selected from the sparse basis library accurately. The spectral reconstruction flowchart based on the DOMP algorithm is shown in Fig. 1.

First, spectral reflectance is processed by principal component analysis to obtain a sparse basis  $B$ . Then a series of initial values are given, and the sparse coefficient  $a$  is returned, based on the DOMP algorithm. Finally, the spectral reflectance  $\hat{r}$  is reconstructed using Eq. (12).

## III. SIMULATIONS

Spectral reflectance reconstruction based on the compressive sensing algorithm is simulated in the MATLAB platform. The standard color card Color Checker Rendition Chart (24) from the GretagMacbeth company is selected as the training sample, and the multispectral reflectance data “young-girl” from the Spectral Color Research Laboratory in the University of Eastern Finland [15] are used to perform the simulation. Standard colorimetric observer spectral tristimulus values of CIE1931 are obtained by multiplying the spectral reflectance

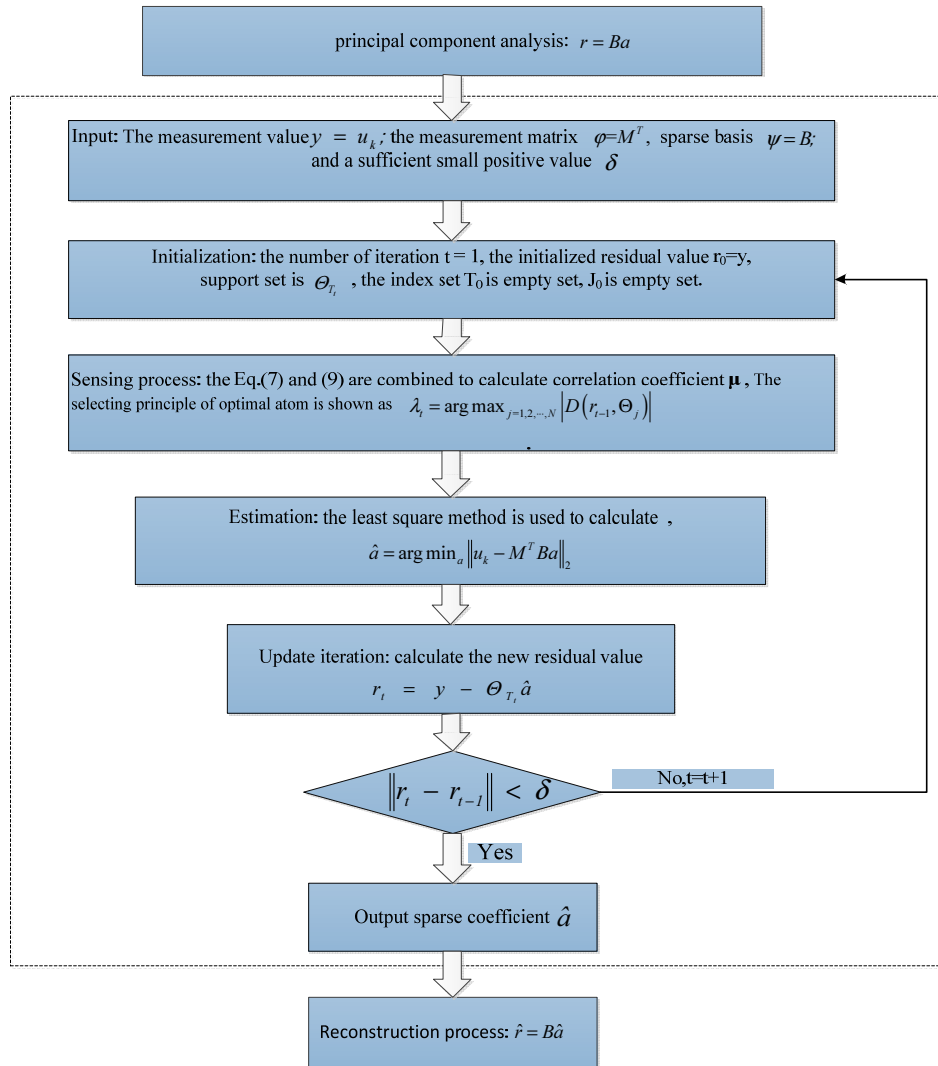


FIG. 1. The flowchart for spectral-reflectance reconstruction.

of multispectral images by the spectral energy distribution matrix of the standard illuminant D50 and CIE1931 standard colorimetric observer spectral matching function. Then, through the known color-space conversion matrix, the CIE1931 standard colorimetric observer spectral tristimulus value is transformed to the corresponding RGB color space value. Finally, the RGB image of the test sample is obtained. The RGB image and three channel values of the image are shown in Fig. 2. The spectral wavelength range is 380-780 nm, the interval is 5 nm, and the spectral reflectance is composed of an 81-dimensional vector.

The process of spectral reflectance reconstruction for “young-girl” is as follows: (1) The basis function vector  $B = (b_1, b_2, b_3)$  is obtained using the principal component analysis algorithm for the spectral reflectance of the training sample (RC24 color card), and  $B$  is used as the basis function vector for spectral-reflectance reconstruction. (2) The transforming matrix  $M^T$  in Eq. (11) consists of the standard illuminant D50 spectral energy distribution matrix, the CIE1931 standard

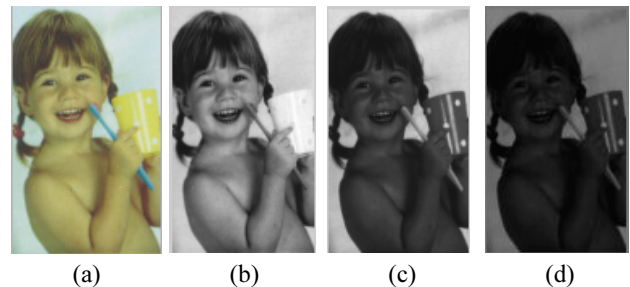


FIG. 2. The RGB image: (a) RGB image, (b) R channel, (c) G channel, (d) B channel.

colorimetric observer spectral matching function, and the matrix for converting CIE1931XYZ color space to RGB color space. The RGB channel response value of “young-girl” is obtained using Eq. (11). (3) Based on the obtained channel response values  $u_k$  for the “young-girl” image, and the first three principal components of the training sample

RC24 color card, the sparse coefficient  $\hat{a}$  of spectral reflectance is obtained by the DOMP algorithm. Then the spectral reflectance of the “young-girl” image is reconstructed using Eq. (12).

The root-mean-square error (RMSE) [16] is used to evaluate the accuracy of spectral reflectance reconstruction, where the original spectral reflectance of each pixel is  $r_i$ , the reconstructed spectral reflectance of each pixel is  $\hat{r}_i$ , and the RMSE is as in Eq. (13):

$$RMSE = \sqrt{\frac{1}{n} \sum_{i=1}^n (r_i - \hat{r}_i)^2} \quad (13)$$

The color difference of the reconstructed spectral reflectance is evaluated using the CIE1976 ( $\Delta E_{ab}$ ) color difference formula [17], for which the coordinate values of the test sample and the reconstructed test sample are  $(L_1, a_1, b_1)$  and  $(L_2, a_2, b_2)$  respectively, and the CIE1976 color difference formula is as in Eq. (14):

$$\Delta E_{ab} = \left[ (L_2 - L_1)^2 + (a_2 - a_1)^2 + (b_2 - b_1)^2 \right]^{1/2} \quad (14)$$

The  $L$  component represents the brightness, the  $a$  component represents the change of chromatic value from green to red, and the  $b$  component represents the change of chromatic value from blue to yellow.

### 3.1. Results and Analysis of Apectral-reflectance Reconstruction Based on the Different Algorithms

Spectral reflectance is reconstructed by different algorithms, based on the pseudo-inverse algorithm (Pinv), Wiener estimation algorithm (Wiener), orthogonal matching pursuit algorithm (OMP), and improved OMP algorithm (DOMP), and it is tested under the standard illuminant D50. The reconstruction errors and color differences are shown in Table 1. The following can be seen from Table 1: (1) The accuracy of the reconstructed spectral reflectance based on the DOMP algorithm is superior to that of the other three algorithms. The RMSE of the reconstructed spectral reflectance is 0.0031, and the maximum value is 0.0735, both less than for the other three methods. (2) The average value of the color difference is 1.3068, and the maximum value is 1.6752, both less than for the other algorithms. This is within the range of human visual experience.

As it is shown in Fig. 3, we can conclude: (1) The accuracy of reconstructed spectral reflectance based on the DOMP algorithm is better than that of the other three kinds of algorithms. (2) Because the spectral reflectance is sparse in its space, the compressive sensing algorithm makes full use of this sparsity, and the accuracy of spectral-reflectance reconstruction for the compressive sensing algorithm based on principal component analysis is higher than for the traditional algorithm. The compressive sensing algorithm based on principal component analysis reduces the computational complexity of the data, and improves the accuracy of reconstruction. (3) In the DOMP algorithm, the Dice coefficient is introduced into the matching criterion between atoms and residual error; thus the optimal atom is matched more quickly and accurately, and the reconstruction accuracy is higher than that of the OMP algorithm.

### 3.2. Effect of the Number of Principal Components on the Accuracy of Spectral-reflectance Reconstruction

The number of principal components of spectral reflectance for the training sample also can affect the spectral-reconstruction accuracy of the test sample. The eigenvalues of the first seven basis function vectors are obtained using the principal component analysis algorithm, and its cumulative contribution is calculated by Eq. (15).  $TV^P$  represents the cumulative contribution of the  $P$  eigenvalues, and  $W_i$  represents the eigenvalues of the  $i_{th}$  principal component.

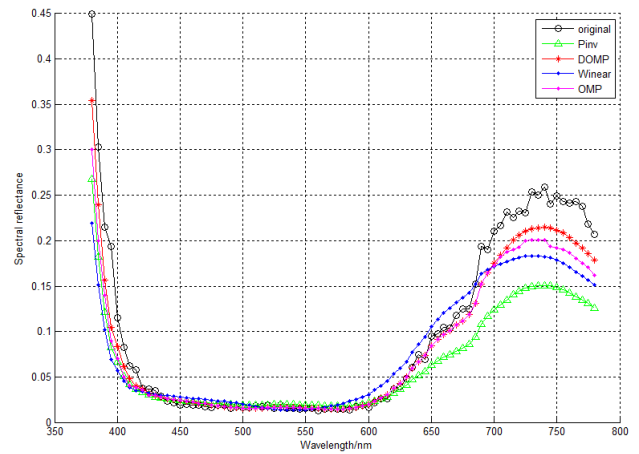


FIG. 3. The reconstructed spectral reflectance from the four algorithms.

TABLE 1. Reconstruction error and color difference for the four methods

methods	RMSE			$\Delta E$		
	Min	Mean	Max	Min	Mean	Max
Pinv	0.0045	0.0090	0.3525	1.2965	1.4397	2.7858
Wiener	0.0010	0.0062	0.2050	0.9850	1.6718	2.3755
OMP	0.00092	0.0050	0.0915	0.8350	1.3951	1.8046
DOMP	0.00035	0.0031	0.0735	0.5135	1.3068	1.6752

$$V^P = \frac{\sum_{i=1}^P W_i}{\sum_{i=1}^n W_i} \quad (15)$$

As it is shown in Table 2, we can conclude: (1) The cumulative contribution increases with the number of principal components; when the number of principal components reaches a certain value, the cumulative contribution changes slowly. (2) The cumulative contribution of the first three eigenvalues is more than 97%, and the that of the first seven is more than 99.7%. When the number of principal components is greater than 3, the growth of cumulative contribution levels off.

The accuracy of spectral-reflectance reconstruction is obtained using Eqs. (13) and (14). The relationship between accuracy of spectral-reflectance reconstruction and the number of principal components is shown in Figs. 4 and 5, from which we can conclude: (1) The root-mean-square error and color difference decrease with increasing number of principal components, so the selection of the number of principal component has some influence on the spectral-reflectance reconstruction. (2) The performance of the DOMP algorithm is better than that of the OMP algorithm. When the number of principal components is the same, the reconstruction error and color difference based on the DOMP algorithm are less than those of the OMP algorithm.

TABLE 2. Eigenvalues and cumulative contribution of the principal components of the RC color card

number	Eigenvalue	contribution
1	3.0741	0.6813
2	1.0051	0.9040
3	0.3135	0.9735
4	0.0616	0.9872
5	0.0277	0.9933
6	0.0135	0.9963
7	0.0069	0.9978

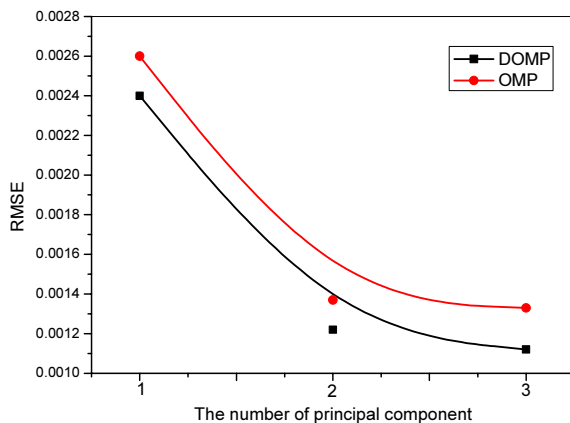


FIG. 4. The relationship between reconstruction error and the number of principal components.

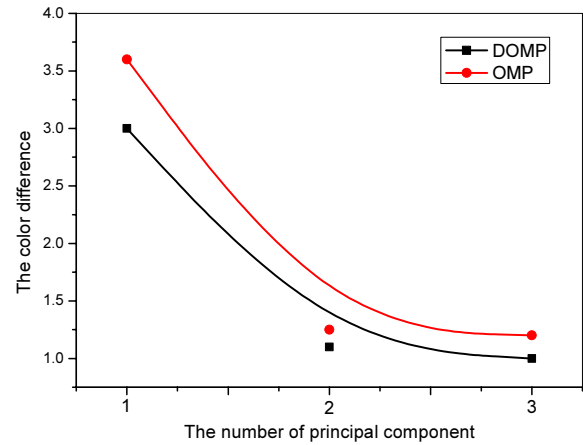


FIG. 5. The relationship between color difference and the number of principal components.

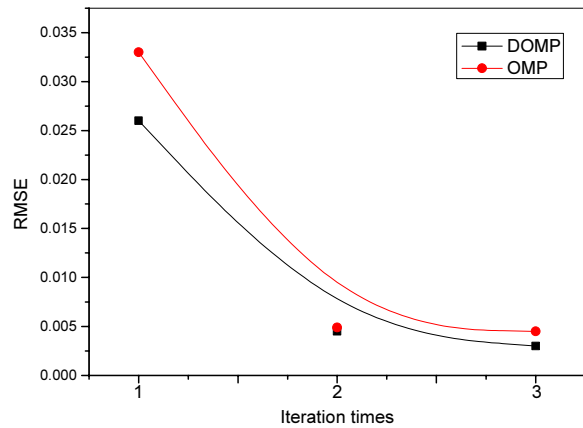


FIG. 6. The relationship of reconstruction error to the number of iterations.

### 3.3. Effect of the Number of Iterations on Spectral-reflectance Reconstruction

The number of iterations affects the accuracy of spectral-reflectance reconstruction based on DOMP and OMP algorithms. The relationship between the root-mean-square error and the number of iterations is shown in Fig. 6, from which we can conclude: (1) The root-mean-square error of reconstruction decreases with increasing number of iterations; when the number of iterations increases to a certain value, the spectral-reconstruction error changes slowly. (2) For a constant number of iterations, the reconstruction error based on the DOMP algorithm is less than that of the OMP algorithm.

## IV. EXPERIMENTAL RESULTS AND ANALYSIS

### 4.1. Data Acquisition

This paper constructs a set of array camera system of multispectral imaging and the array camera uses three colored



CCD digital camera and three filters to compose a multispectral digital camera. The output image channel value is shown as Eq. (4), and the process of spectral imaging is shown in Fig. 7. The ENVI software is used to process the obtained spectral image. Spectral reflectance is measured by an Eyeone spectrophotometer, under conditions of the CIE standard D65 light source and  $2^\circ$  field of view. The conversion matrix  $M'$  is obtained from the channel value and the spectral reflectance of the RC24 color card. The test sample selects ColorChecker SG (140), and its channel response value is obtained by the spectral imaging system; then the spectral reflectance of each pixel of the SG color card is reconstructed by combining the conversion matrix  $M'$  and the channel response value. The reconstructed spectral reflectance is compared to the original. The original image of the RC24 color card is shown in Fig. 8, and the absolute spectrum (multichannel response values) of one pixel of the RC24 color card is shown in Fig. 9.

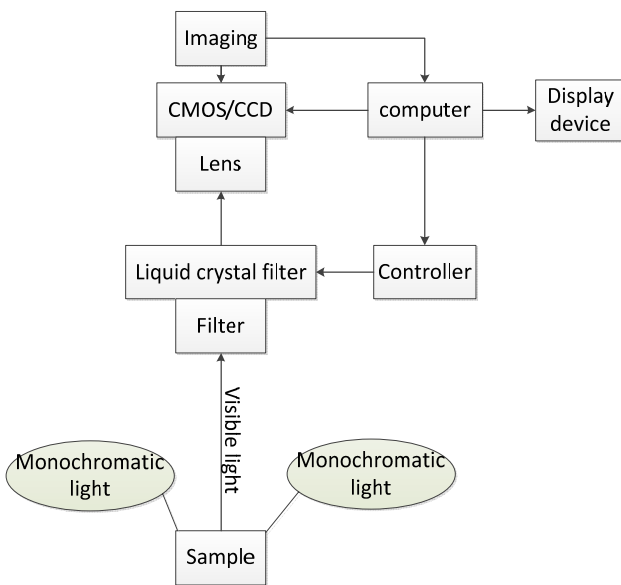


FIG. 7. Flowchart for spectral imaging.

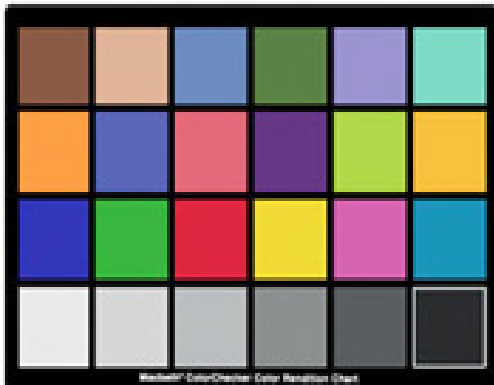


FIG. 8. Image of the RC-24 color card.

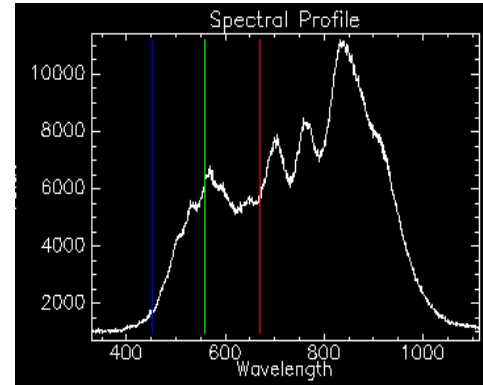


FIG. 9. The spectrum of a pixel.

#### 4.2. Spectral-reflectance Reconstruction Based on Different Algorithms

There are six channel-response values for each sample in our experiment, which is different from the three channel-response values obtained by simulation. To make the results more adequate, there are some results comparison by experiment. A pixel of the test sample is selected, and the accuracy of spectral reconstruction based on the pseudo-inverse method, Wiener estimation method, OMP algorithm, and DOMP algorithm is compared. The root-mean-square errors and color differences of spectral reflectance based on different algorithms versus experiment are shown in Table 3. From Table 3 we can conclude: (1) The accuracy of spectral-reflectance reconstruction based on the DOMP algorithm is superior to that based on the other methods, and the root-mean-square error based on DOMP is 0.0010, which is lower than that for the other three algorithms. (2) The color difference by DOMP is 1.57, which is much smaller than that by the other algorithms. The reconstruction of spectral reflectance based on the DOMP algorithm can greatly improve the accuracy of color reappearance. (3) The computational time for the DOMP algorithm is 3.70 seconds, which is less than that of the other three algorithms. The important parts of the residual error are pinpointed rapidly and accurately by the DOMP algorithm, so the computational time is less by DOMP than by OMP.

A pixel of the test sample SG color card is selected, and its spectral reflectance is reconstructed by the Wiener estimation method, pseudo-inverse method, OMP algorithm, and DOMP algorithm. As it is seen in Fig. 10, we can conclude: (1) The accuracy of spectral-reflectance reconstruction based on the DOMP algorithm is greater than that of the other three kinds of algorithms. For the wavelength range of about 580 nm to 700 nm, the reconstruction effect is not obvious, because there is some influence of system noise and the external environment. (2) The pseudo-inverse method uses the least-squares method to reconstruct the spectral reflectance; the reconstruction accuracy is affected by the modulus of the observed value, and the calculated amount increases with the increase of the observed value.

TABLE 3. The reconstruction accuracy of the four algorithms

Method	RMSE	$\Delta E$	Time (s)
Pinv	0.0343	2.35	18.20
Wiener	0.0245	1.97	13.70
OMP	0.0087	2.05	8.40
DOMP	0.0010	1.57	3.70

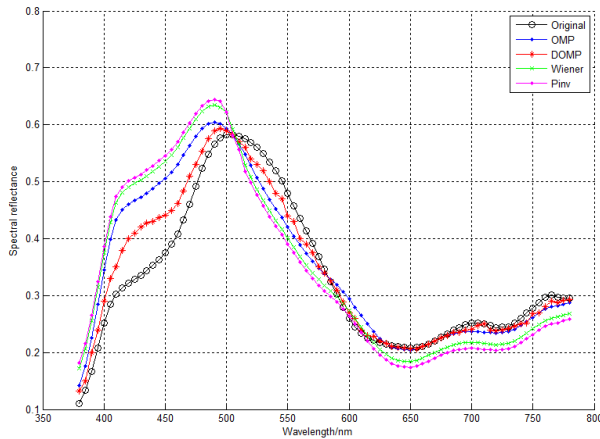


FIG. 10. Spectral-reflectance reconstruction curves for the different algorithms.

Thus when the number of observations is limited, it is difficult to accurately reconstruct the reflectance of the image's surface.

## V. CONCLUSION

The traditional algorithm for spectral reconstruction uses the pseudo-inverse model to reconstruct the spectral reflectance of a test sample, and the accuracy of reconstruction is not high. The spectral reflectance is sparse in space, but the traditional spectral-reconstruction algorithm does not make full use of this sparsity. The compressive sensing algorithm, however, can make full use of the sparsity of the spectral reflectance. The computing time is reduced, as is the amount of calculation. Therefore, this paper proposes a new compressive sensing algorithm for reconstructing spectral reflectance. In this paper, first the dimension of the spectral reflectance is reduced through principal component analysis, and then the basis function vector of spectral reflectance is obtained. Second, on the basis of analyzing the orthogonal matching pursuit algorithm, a new algorithm based on the Dice matching criterion is proposed. The Dice similarity coefficient is introduced to calculate the correlation coefficient of an atom and the residual error, and used to select atoms from an atom library. Then the sparse coefficient is obtained. Finally, the spectral reflectance of the test sample is reconstructed through the first three principal components and the sparse coefficient.

In this paper, on the basis of analyzing compressive sensing based on the orthogonal matching pursuit algorithm, a new algorithm based on the Dice matching criterion is proposed. The accuracy of spectral reconstruction based on the pseudo-inverse method, the Wiener estimation method, the OMP algorithm, and the DOMP algorithm is compared via simulation on the MATLAB platform, and via experiment. The result is that spectral-reconstruction accuracy based on the DOMP algorithm is higher than that based on the other three algorithms. The number of principal components of spectral reflectance for the training sample obtained by the PCA method can affect the spectral-reconstruction accuracy for the test sample. The root-mean-square error and color difference decreases with increasing number of principal components. The number of iterations also affects the accuracy of spectral-reflectance reconstruction, and reconstruction error decreases with increasing number of iterations.

Spectral-reflectance reconstruction based on the DOMP algorithm can effectively improve the accuracy of color-information replication, and high-accuracy color-information reproduction can be realized.

## ACKNOWLEDGMENT

This study is supported by the National Basic Research Program of China (973 Program) (Grant No.2015CB352004), the National Natural Science Foundation of China (Grant No. 61405115, 61378035), the Natural Science Foundation of Shanghai (Grant No. 14ZR1428400), and the Innovation Project of Shanghai Municipal Education Commission (Grant No. 14YZ099).

## REFERENCES

1. B. W. Jiang, "Method of multi-spectral images reduce-dimensions based on PCA," *Inform. Technol.* **8**, 98-101 (2012).
2. D. Y. Tzeng and R. S. Berns, "A review of principal component analysis and its applications to color technology," *Color Res. Appl.* **30**, 84-98 (2005).
3. C. James and A. Gibson, "Temporally constrained ICA: an application to artifact rejection in electromagnetic brain signal analysis," *IEEE Trans. Biomed. Eng.* **50**, 1108-1116 (2003).
4. K. Takase, N. Tsumura, T. Nakaguchi, and Y. Miyake, "Fast estimation algorithm for calculation of reflectance map based on wiener estimation technique," *Opt. Rev.* **12**, 20-24 (2005).
5. H. L. Shen, H. J. Wan, and Z. C. Zhang, "Estimating reflectance from multispectral camera responses based on partial least-squares regression," *Electron. Imaging* **19**, 205-212 (2010).
6. J. Romberg, "Imaging via compressive sampling," *IEEE Signal Process. Mag.* **25**, 14-20 (2008).
7. D. L. Donoho, "Compressed sensing," *IEEE Trans. Inform. Theory* **52**, 1289-1306 (2006).
8. S. H. Amirshahi and S. A. Amirshahi, "Adaptive non- negative



- bases for reconstruction of spectral data from colorimetric information," *Opt. Rev.* **17**, 562-569 (2010).
9. E. Candès, J. Romberg, and T. Tao, "Stable signal recovery from incomplete and inaccurate measurements," *Comm. Pure Appl. Math.* **59**, 1207-1223 (2006).
  10. E. Candès, J. Romberg, and T. Tao, "Robust uncertainty principles: Exact signal reconstruction from highly incomplete frequency information," *IEEE Trans. Inform. Theory* **52**, 489-509 (2006).
  11. L. H. Zhang, D. Liang, Z. L. Pan, and X. H. Ma, "Study on the key technology of reconstruction spectral reflectance based on the algorithm of compressive sensing," *Opt. Quant. Electron.* **47**, 1679-1692 (2015).
  12. J. A. Tropp and A. J. Gilbert, "Signal recovery from random measurements via orthogonal matching pursuit," *IEEE Trans. Inform. Theory* **53**, 4655-4666 (2007).
  13. E. Candès, J. Romberg, and T. Tao, "Stable signal recovery from incomplete and inaccurate measurements," *Comm. Pure Appl. Math.* **59**, 1207-1223 (2006).
  14. J. Bioucas-Dias and M. Figueiredo, "A new TwIST: two-step iterative shrinkage/thresholding for image restoration," *IEEE Trans. Image Process.* **16**, 2992-3004 (2007).
  15. Spectral Image Database, University of Eastern Finland Color Group[EB/OL]. <http://www.uef.fi/en/web/spectral>
  16. P. Stigell, K. Miyata, and M. Hauta-Kasari, "Wiener estimation method in estimating of spectral reflectance from RGB images," *Pattern Recognit. Image Anal.* **17**, 233-242 (2007).
  17. K. McLaren, "The development of the CIE 1976 (L\*a\*b\*) uniform colour-space and colour-difference formula," *Coloration Technology* **92**, 338-341 (2008).